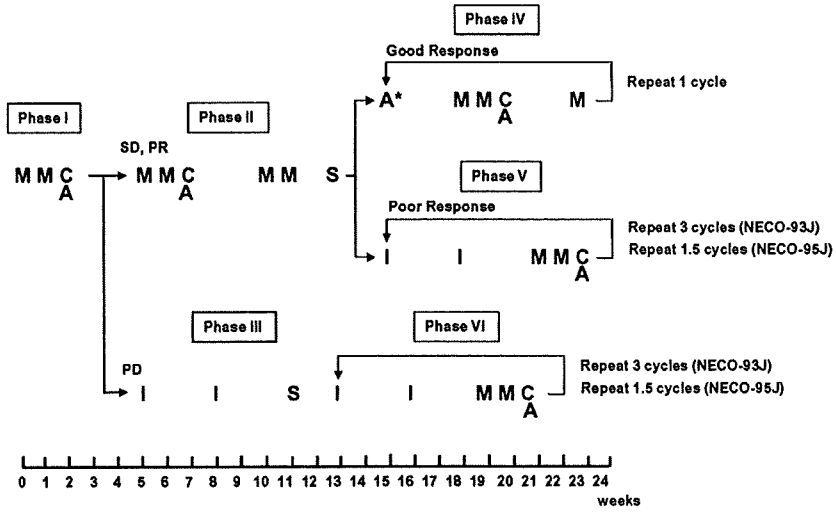

Fig. 1. Chemotherapy for the Neoadjuvant Chemotherapy for Osteosarcoma (NECO) study. During phases V and VI the regimens were repeated for three cycles (total four cycles) for NECO-93J and 1.5 cycles (total 2.5 cycles) for NECO-95J. *M*, high-dose methotrexate 8–12 g/m^2; *C*, cisplatinum 120 mg/m^2; *A*, adriamycin 60 mg/m^2 × 2 days; *A**, adriamycin 90 mg/m^2 × 3 days; *I*, high-dose ifosfamide 16 g/m^2 × 7 days; *S*, surgery

Postoperative adjuvant chemotherapy

For patients with tumors assessed as SD or PR after the preoperative phase I chemotherapy, if the histological response to preoperative chemotherapy was evaluated as a good response (i.e., ≥90% tumor necrosis was obtained), a course of ADR (30 mg/m^2/day × 3 days), three courses of HD-MTX, and a course of CDDP and ADR were given as postoperative chemotherapy. The same regimen was then repeated (phase IV). If the histological response was evaluated as poor (i.e., <90% tumor necrosis was achieved), two courses of HD-IFO, two courses of HD-MTX, and a course of CDDP and ADR were given. The same postoperative regimen was repeated for total of four cycles (phase V).

For patients with tumors assessed as PD after preoperative chemotherapy, the postoperative chemotherapy was carried out the same as the phase V regimen described above (i.e., eight courses of HD-IFO, eight courses of HD-MTX, and four courses of CDDP and ADR) (phase VI). No additional therapy was given until the patient had treatment failure, which included local recurrence and/or distant metastasis.

Chemotherapy regimen for NECO-95J

Preoperative chemotherapy in the NECO-95J study was the same as the NECO-93J regimen. The surgical treatment and histological evaluation for tumor necrosis were also performed in the same way as in NECO-93J. The postoperative chemotherapy in NECO-95J regimen, however, was shortened to six courses of HD-IFO, four courses of HD-MTX, and two courses of CDDP and ADR during phases V and VI (Fig. 1).

Evaluation of response to preoperative chemotherapy

For both regimens, patients were assessed for their clinical response to the induction chemotherapy when phase I chemotherapy was completed. The response was evaluated using MRI, CT, and/or plain radiography of the primary tumor.

The definitions of the clinical response were as follows: complete response (CR), total disappearance of the tumor; partial response (PR), decrease in the diameter of the extramedullary lesion or induction of sclerotic change in the intramedullary lesion; no change (NC), no changes in the diameter of the extramedullary lesion and the appearance of an intramedullary lesion; progressive disease (PD), increase in the diameter of extramedullary and/or intramedullary lesions or appearance of a new lesion.

The pathological response was evaluated using the resected tumors as previously described but with some modification.[8] The response was defined as follows: complete response (grade 3 response), total necrosis of the tumor; partial response (grade 2 response), ≥90% necrosis in the tumor; minor response (grade 1 response), ≥50% but <90% necrosis in the tumor; no response (grade 0 response), <50% necrosis of the tumor. The pathological response rate was defined as the percentage of patients who achieved a complete or partial pathological response after the preoperative chemotherapy.

Toxicity

Regimen-related toxicity was graded according to the Japan Clinical Oncology Group (JCOG) common toxicity criteria, where grade 3 indicates severe toxicity,

grade 4 life-threatening toxicity, and grade 5 lethal toxicity.

Statistical analysis

Survival was calculated using the Kaplan-Meier method with standard errors. Overall survival (OAS) was calculated from the date of entry into the study until death of any cause. Event-free survival (EFS) was calculated from the date of entry until the first event (i.e., recurrence or progress of the disease or death of any cause). The generalized Peto and Peto Wilcoxon test was used to compare survival curves.

Results

Patient characteristics

The characteristics of the 113 eligible patients are summarized in Table 1. Among 124 patients with osteosarcoma, 11 were excluded from the analyses as described above. For NECO-93J, a total of 55 patients were registered, 50 of whom were included in the analyses. Five patients were ineligible: two because of metastasis; one age >30 years; one had insufficient organ function; and in one the tumor arose in the trunk. For the NECO-95J study, 69 patients were recruited, 63 of whom were eligible. Six patients were excluded: four due to metastasis; one for age >30 years; and in one the tumor arose in the trunk. The mean follow-up period for all patients was 75.6 months (range 11–140 months).

Response

A total of 49 patients were assessable for their response to preoperative chemotherapy in the NECO-93J trial, as one patient dropped out of the regimen during phase I chemotherapy and thus was not evaluated for a response. After phase I therapy, the tumors of 11 patients (22.4%) were evaluated as PD, and HD-IFO was given at the following chemotherapy session (phase VI). In all, 38 patients did not exhibit disease progression and were treated as in the phase II arm. One of the 38 dropped out from the regimen during phase II, and 22 and 15 patients were treated in phases IV and V, respectively. The pathological response using surgical specimens was evaluated in 48 patients. A grade 2 or 3 response was achieved in 20 (41.7%) patients.

In the NECO-95J trial, 61 patients were evaluable for a response to preoperative chemotherapy; two patients had dropped out during phase I chemotherapy. After phase I, the tumors of 11 (18.0%) patients were evaluated as PD. Two patients dropped out of the regimen during phase II, and 25 and 23 patients were treated during phases IV and V, respectively. The pathological response using surgical specimens was evaluated in 61 patients. A grade 2 or 3 response was achieved in 26 (42.6%) patients. For all patients, the pathological response rate to the preoperative chemotherapy was 42.2% (46/109) (Table 2).

Table 2. Pathological response to NECO regimen

Response	No. of patients		
	NECO-93J	NECO-95J	Total
Grade 0	7	10	17 (15.6%)
Grade 1	21	25	46 (42.2%)
Grade 2	12	23	35 (32.1%)
Grade 3	8	3	11 (10.1%)
Total	48	61	109 (100%)

Table 1. Patients' characteristics

Parameter	NECO-93J	NECO-95J	Total
Patients (no.)	50	63	113
Age (years), mean/range	15.3 (6–26)	14.8 (6–27)	15.0 (6–27)
Sex			
Male	27	44	71
Female	23	19	42
Osteosarcoma site			
Femur	29	33	62
Tibia	13	20	33
Humerus	5	5	10
Fibula	3	3	6
Others	0	2	2
Osteosarcoma subtype			
Osteoblastic	37	51	88
Chondroblastic	6	5	11
Fibroblastic	3	3	6
Others	4	4	8

NECO, Neoadjuvant Chemotherapy for Osteosarcoma (study)

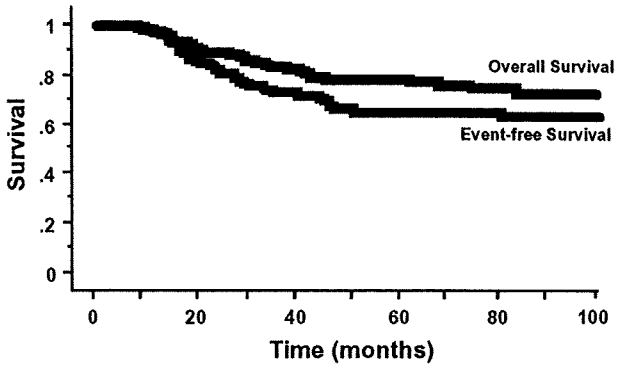

Fig. 2. Kaplan-Meier curves of event-free and overall survival for all patients in the NECO study

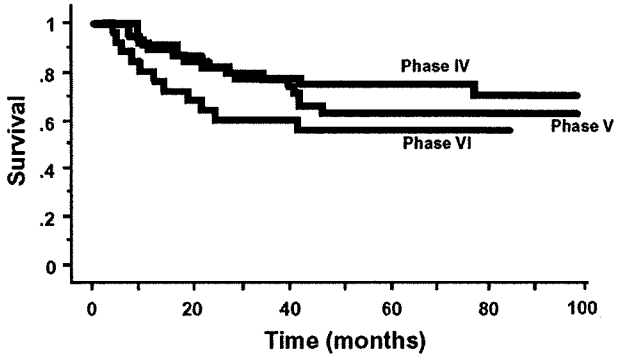

Fig. 3. Kaplan-Meier curves of event-free survival (EFS) according to chemotherapy phases in the NECO study. The differences between EFS rates for phases IV, V, and VI were not significant

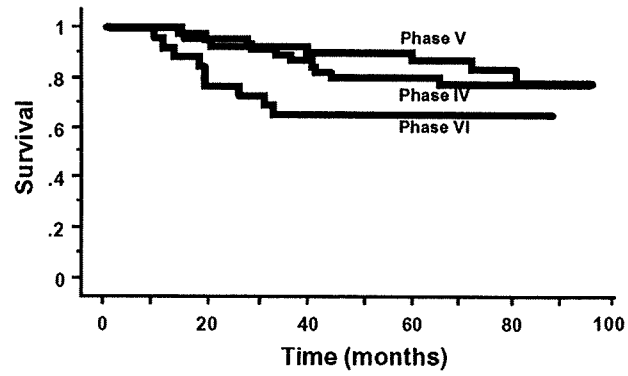

Fig. 4. Kaplan-Meier curves of overall survival (OAS) according to chemotherapy phases in the NECO study. The differences between OAS rates for phases IV, V, and VI were not significant

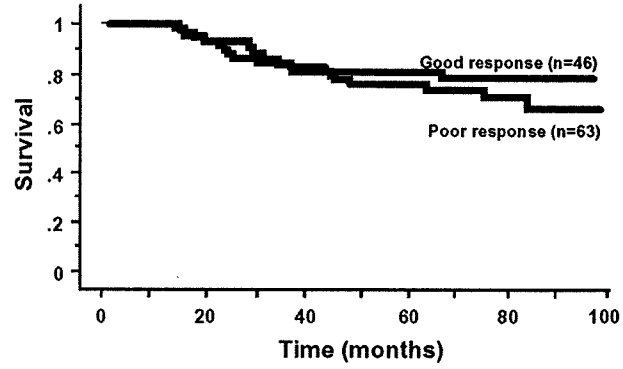

Fig. 5. Kaplan-Meier curves of overall survival (OAS) according to pathological responses in NECO study. The difference between OAS rates for each group was not significant

Event-free survival

The 5-year EFS for all 113 patients in the NECO study was 65.5% ± 4.5% (Fig. 2). The 5-year EFS for the chemotherapy phases in the NECO regimen were 74.5% ± 6.4% for phase IV ($n = 47$), 63.2% ± 7.8% for phase V ($n = 38$), and 59.1% ± 10.5% for phase VI ($n = 22$) (Fig. 3). The differences in the EFS rates among phases in the NECO study were not significant.

The 5-year EFS for 50 patients in the NECO-93J trial was 51.9% ± 7.1%, whereas for 63 patients treated with NECO-95J it was 76.2% ± 5.4%. This result is significantly better than that with NECO-93J ($P = 0.019$).

Overall survival

The 5-year OAS for 113 patients in the NECO study was 77.9% ± 3.9% (Fig. 2). Among these patients, 31 had died by the final follow-up, and 25 of the 31 died of their disease (DOD). The 5-year OAS rates for the chemotherapy phases in the NECO regimen were 78.7% ± 6.0% for phase IV ($n = 47$), 89.5% ± 5.0% for phase V ($n = 38$), and 68.2% ± 9.9% for phase VI ($n = 22$). The differences in OAS among the phases in the NECO study were not significant (Fig. 4).

The 5-year OAS rates for patients with a good response to neoadjuvant chemotherapy ($n = 46$) and for those with a poor response ($n = 63$) were 82.6% ± 5.6% and 77.5% ± 5.3%, respectively. The difference in OAS between pathological responses in the NECO study was not significant ($P = 0.357$) (Fig. 5). These results suggest that poor respondents might be rescued by the addition of IFO.

The 5-year OAS for 50 patients treated with NECO-93J was 72.0% ± 6.3% (Fig. 6). The 5-year OAS rates for each phase in the NECO-93J trial were 63.6% ± 10.3% for phase IV ($n = 22$), 86.2% ± 9.1% for phase V ($n = 15$), and 72.7% ± 13.4% for phase VI ($n = 11$). The differences in OAS among phases in NECO-93J were not significant.

The 5-year OAS for 63 patients treated with NECO-95J was 82.5% ± 4.8% (Fig. 6). Although the difference

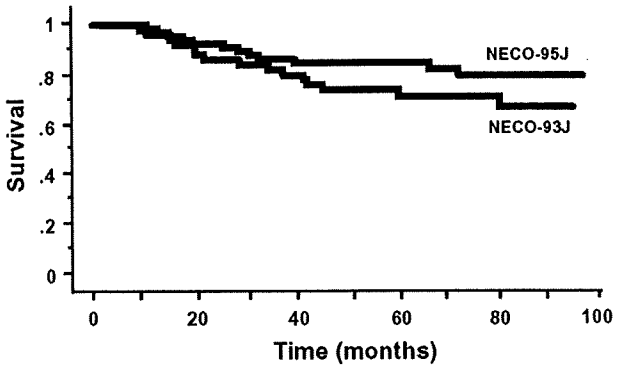

Fig. 6. Kaplan-Meier curves of overall survival for the NECO-93J and NECO-95J studies

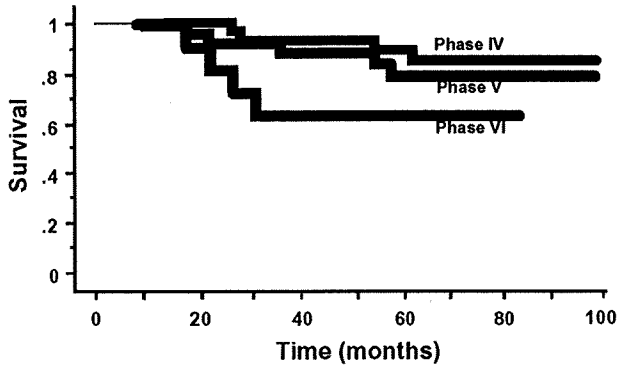

Fig. 7. Kaplan-Meier curves of overall survival according to chemotherapy phases in the NECO-95J study. The differences between OAS rates for phases IV, V, and VI were not significant

in the OAS rate between the two regimens was not significant, NECO-95J tended to have a more favorable OAS. The 5-year OAS rates for each phase in NECO-95J were 92.0% ± 5.4% for phase IV ($n = 25$), 82.1% ± 8.1% for phase V ($n = 23$), and 63.6% ± 14.5% for phase VI ($n = 11$) (Fig. 7). The differences in OAS among phases in NECO-95J were not significant.

Local control

Surgical resection was performed in 110 of the 113 eligible patients in the NECO study. Amputation was carried out in 10 patients, whereas limb salvage surgery and rotation plasty were done in 90 and 10 patients, respectively. The limb-sparing rate was 90.9% in this series. The surgical margins achieved were a curative margin in 32 (29.1%) patients, a wide margin in 75 (68.2%) patients, a marginal margin in 2 (1.8%) patients, and an intralesional margin in 1 (0.9%) patient. A sufficiently wide margin was obtained in 97.3% of the operated patients. Local recurrence was observed in four patients, and the local recurrence rate was low (3.6%). Two of the three patients whose surgical margins were marginal or intralesional experienced a local recurrence.

Toxicity

Of the 113 patients, 6 (5.3%) died of another cause (DOC): cardiomyopathy induced by ADR (3), infection (1), secondary leukemia (1), regimen-related toxicity (1). Toxicity information was available for a total of 882 courses of chemotherapy. Grade 3 and 4 hematopoietic toxicity was found during 277 courses (31.4%). During the courses with HD-IFO and CDDP + ADR, grade 3 and 4 hematopoietic toxicity was frequent (74.0% and 50.8%, respectively). Grade 3 and 4 nonhematopoietic toxicities were found during 198 courses (22.4%). The nonhematopoietic toxicities included gastrointestinal disorders (6.3%), liver dysfunction (14.3%), electrolyte abnormalities (0.6%), neurological toxicity (0.3%), and infection (0.2%).

Regarding treatment compliance, all chemotherapy was completed in 22 of 50 patients (44.0%) in NECO-93J. A total of 17 (77.3%) patients received all chemotherapy scheduled during phase IV, whereas only 3 (20.0%) in phase V and 2 (18.2%) in phase VI did so. The treatment compliance rate was low during the phases using IFO. The most frequent reason for patients not receiving the whole treatment protocol was hematopoietic toxicity. In NECO-93J, the patients received an average of two (2.0) chemotherapy cycles during phases V and VI. Therefore, in NECO-95J we reduced the number of chemotherapy cycles during phases V and VI to improve compliance with the chemotherapy. Consequently, in the NECO-95J study, 43 of 63 (68.3%) patients took all of the chemotherapy: 23 (92.0%) during phase IV, 14 (60.9%) during phase V, and 6 (54.5%) during phase VI. The most frequent reason for patients not undergoing all of the treatment protocol was patient refusal.

Regimen compliance did not affect the prognosis of patients in the NECO-93J study. The 5-year OAS of the patients who completed all chemotherapy and those not receiving all chemotherapy, respectively, were 52.9% and 100% for phase IV, 100% and 91.7% for phase V, and 100% and 66.7% for phase VI. The differences in OAS between the two groups for all phases were not significant. In NECO-95-J, the 5-year OAS of the patients receiving all chemotherapy and those not receiving all chemotherapy were, respectively, 91.3% and 100% for phase IV, 85.7% and 88.9% for phase V, and 83.3% and 40.0% for phase VI. The differences in OAS regarding regimen compliance during all phases in NECO-95J were not significant.

Discussion

The survival of patients with osteosarcoma has been dramatically improved by intensive systemic chemotherapy and surgery for operable disease.[4–10] However, the treatment strategies are still not successful in approximately 30%–40% of patients with localized osteosarcoma in the extremities. To improve the outcome of the multimodal therapies for the tumor, it is necessary to improve the efficacy of the chemotherapy by better use of antitumor drugs, including HD-MTX, ADR, CDDP, and IFO. Because these drugs are thought to be the most active for osteosarcoma, neoadjuvant and adjuvant chemotherapies that include them are the current standard regimens worldwide. For Japanese patients with osteosarcoma, however, only a few retrospective studies have been reported, and they were from single institutions.[16–18]

To evaluate the efficacy of chemotherapy for osteosarcoma in Japan, we conducted the first prospective, multiinstitutional trial of neoadjuvant chemotherapy for osteosarcoma, the NECO study. The 5-year EFS and OAS rates for 113 patients with operable, nonmetastatic osteosarcoma of the extremities treated by the NECO regimen were 65.5% and 77.9%, respectively. The outcome of the present study was comparable to those of recent studies reported from the United States and Europe.[4–10] In this regard, however, it is noteworthy that the patients enrolled in NECO were under age 30 years, whereas in many studies carried out in the United States and Europe the inclusion criterion on age has been under 40 years.[12–14,19–21] As the age of the patients with osteosarcoma is a significant prognostic factor, the relatively younger population recruited in the NECO trial might have produced the favorable results of this trial.

In the first protocol, NECO-93J, the 5-year EFS and OAS rates were 51.9% and 72.0%, respectively. NECO-93J aimed to rescue the patients who did not respond to the preoperative chemotherapy by alternating intensive chemotherapy with HD-IFO (phases V and VI), as shown in Fig. 1. However, the regimen containing HD-IFO was highly toxic, and only 20.0% and 18.2% of the patients, respectively, received all chemotherapy during phases V and VI. When we compared the survival of patients treated with the entire chemotherapy protocol versus those who were not, the difference was not significant (data not shown). Because the patients received a mean of only two (2.0) cycles of chemotherapy during phases V and VI in NECO-93J, we shortened the postoperative chemotherapy in NECO-95J to improve compliance with the regimen. Consequently, in the NECO-95J study, the rates of patients who completed the entire treatment protocol during phases V and VI were, respectively, 60.9% and 54.5%. Despite the reduction of cycles with HD-IFO, the outcome was improved in NECO-95J; the 5-year EFS and OAS rates were 76.2% and 82.5%, respectively. However, further improvement of treatment compliance is necessary.

In the present study, 22 of 113 patients (19.5%) had tumors that were evaluated as PD after preoperative chemotherapy. The PD rate in the NECO trial was relatively high, whereas the PD rates in other trials varied from 0% to about 20%.[12,15,19,21] Thus, the results suggest that the induction chemotherapy in our study should be more intensive to suppress the PD rate. In the present study, however, the clinical response to the induction chemotherapy was evaluated when phase I chemotherapy was completed (i.e., when two courses of HD-MTX and a course of CDDP + ADR had been given). The patients evaluated as having PD were treated with HD-IFO during the following chemotherapy cycle (phase VI), and the EFS and OAS rates for the patients treated in the phase VI arm were 59.1% ± 10.5% and 68.2% ± 9.9%, respectively. There were no significant differences between survival rates for patients with tumors assessed as PD or not PD. These observations suggest that the prognosis of the patients evaluated as having PD might be improved by addition of HD-IFO to the regimen. However, there is the possibility that the evaluation of PD had been done too early, which subsequently led to underestimating the effect of the preoperative induction chemotherapy. This possibility should be excluded to conclude that HD-IFO could be effective for the patients who did not respond to HD-MTX, CDDP, and ADR.

The significance of adding IFO to HD-MTX and CDDP + ADR has been controversial, although IFO is thought to be active against osteosarcoma.[6,10,12–15] Several studies have reported that application of IFO to patients who exhibit a poor response to preoperative chemotherapy using HD-MTX, CDDP, and ADR did not improve their prognosis. The IFO doses used in the studies were relatively low (4.5–9.0 g/m^2).[6,10,20] On the other hand, successful results after IFO addition have also been reported. In the clinical studies IOR/OS-N2 and IOR/OS-N3, the prognosis of poor responders to preoperative chemotherapy using HD-MTX, CDDP, and ADR was improved by adding high-dose IFO (10 g/m^2).[19,22] The dose of IFO used in the present study (16 g/m^2/course, 96–128 g/m^2 total) was higher than that in other studies. These results suggest that high doses of IFO (>10 g/m^2) might be crucial for improving the outcome of patients with a poor response to preoperative chemotherapy. Randomized clinical trials are needed to elucidate this possibility. A large randomized study, EURAMOS1, has been started in Europe and the United States to test whether the addition of high-dose IFO can improve the prognosis of patients with a poor response to preoperative chemotherapy. We are

also planning to perform a randomized clinical trial to confirm the results of the present study.

Acknowledgments. The authors express sincere appreciation to all members of the Japan Bone Tumor Chemotherapy Study Group. We also thank M. Sekiya (Wyeth K.K. Japan) for kind assistance with the data collection and analyses. The study was supported in part by a Grant-in-Aid for Cancer Research from the Ministry of Health, Labor and Welfare, Japan.

References

1. Rosen G, Marcove RC, Huvos AG, Caparros BI, Lane JM, Nirenberg A, et al. Primary osteogenic sarcoma: eight-year experience with adjuvant chemotherapy. J Cancer Res Clin Oncol 1983;106(suppl):55–67.
2. Link MP, Goorin AM, Miser AW, Green AA, Pratt CB, Belasco JB, et al. The effect of adjuvant chemotherapy on relapse-free survival in patients with osteosarcoma of the extremity. N Engl J Med 1986;314:1600–6.
3. Eilber F, Giuliano A, Eckardt J, Patterson K, Moseley S, Goodnight J. Adjuvant chemotherapy for osteosarcoma: a randomized prospective trial. J Clin Oncol 1987;5:21–6.
4. Goorin AM, Schwartzentruber DJ, Devidas M, Gebhardt MC, Ayala AG, Harris MB, et al. Presurgical chemotherapy compared with immediate surgery and adjuvant chemotherapy for nonmetastatic osteosarcoma: Pediatric Oncology Group Study POG-8651. J Clin Oncol 2003;21:1574–80.
5. Bacci G, Bertoni F, Longhi A, Ferrari S, Forni C, Biagini R, et al. Neoadjuvant chemotherapy for high-grade central osteosarcoma of the extremity: histologic response to preoperative chemotherapy correlates with histologic subtype of the tumor. Cancer 2003;97:3068–75.
6. Patel SJ, Lynch JW Jr, Johnson T, Carroll RR, Schumacher C, Spanier S, et al. Dose-intense ifosfamide/doxorubicin/cisplatin based chemotherapy for osteosarcoma in adults. Am J Clin Oncol 2002;25:489–95.
7. Wilkins RM, Cullen JW, Odom L, Jamroz BA, Cullen PM, Fink K, et al. Superior survival in treatment of primary nonmetastatic pediatric osteosarcoma of the extremity. Ann Surg Oncol 2003;10:498–507.
8. Bielack SS, Kempf-Bielack B, Delling G, Exner GU, Flege S, Helmke K, et al. Prognostic factors in high-grade osteosarcoma of the extremities or trunk: an analysis of 1,702 patients treated on neoadjuvant cooperative osteosarcoma study group protocols. J Clin Oncol 2002;20:776–90.
9. Crews KR, Liu T, Rodriguez-Galindo C, Tan M, Meyer WH, Panetta JC, et al. High-dose methotrexate pharmacokinetics and outcome of children and young adults with osteosarcoma. Cancer 2004;100:1724–33.
10. Meyers PA, Schwartz CL, Krailo M, Kleinerman ES, Betcher D, Bernstein ML, et al. Osteosarcoma: a randomized, prospective trial of the addition of ifosfamide and/or muramyl tripeptide to cisplatin, doxorubicin, and high-dose methotrexate. J Clin Oncol 2005;23:2004–11.
11. Hauben EI, Weeden S, Pringle J, Van Marck EA, Hogendoorn PC. Does the histological subtype of high-grade central osteosarcoma influence the response to treatment with chemotherapy and does it affect overall survival? A study on 570 patients of two consecutive trials of the European Osteosarcoma Intergroup. Eur J Cancer 2002;38:1218–25.
12. Souhami RL, Craft AW, Van der Eijken JW, Nooij M, Spooner D, Bramwell VH, et al. Randomised trial of two regimens of chemotherapy in operable osteosarcoma: a study of the European Osteosarcoma Intergroup. Lancet 1997;350:911–7.
13. Bramwell VH, Burgers M, Sneath R, Souhami R, van Oosterom AT, Voute PA, et al. A comparison of two short intensive adjuvant chemotherapy regimens in operable osteosarcoma of limbs in children and young adults: the first study of the European Osteosarcoma Intergroup. J Clin Oncol 1992;10:1579–91.
14. Bacci G, Briccoli A, Ferrari S, Longhi A, Mercuri M, Capanna R, et al. Neoadjuvant chemotherapy for osteosarcoma of the extremity: long-term results of the Rizzoli's 4th protocol. Eur J Cancer 2001;37:2030–9.
15. Zalupski MM, Rankin C, Ryan JR, Lucas DR, Muler J, Lanier KS, et al. Adjuvant therapy of osteosarcoma — a phase II trial: Southwest Oncology Group study 9139. Cancer 2004;100: 818–25.
16. Wada T, Isu K, Takeda N, Usui M, Ishii S, Yamawaki S. A preliminary report of neoadjuvant chemotherapy NSH-7 study in osteosarcoma: preoperative salvage chemotherapy based on clinical tumor response and the use of granulocyte colony-stimulating factor. Oncology 1996;53:221–7.
17. Uchida A, Myoui A, Araki N, Yoshikawa H, Shinto Y, Ueda T. Neoadjuvant chemotherapy for pediatric osteosarcoma patients. Cancer 1997;79:411–5.
18. Tsuchiya H, Tomita K, Mori Y, Asada N, Morinaga T, Kitano S, et al. Caffeine-assisted chemotherapy and minimized tumor excision for nonmetastatic osteosarcoma. Anticancer Res 1998;18: 657–66.
19. Bacci G, Ferrari S, Bertoni F, Ruggieri P, Picci P, Longhi A, et al. Long-term outcome for patients with nonmetastatic osteosarcoma of the extremity treated at the Istituto Ortopedico Rizzoli according to the Istituto Ortopedico Rizzoli/Osteosarcoma-2 protocol: an updated report. J Clin Oncol 2000; 18:4016–27.
20. Smeland S, Muller C, Alvegard TA, Wiklund T, Wiebe T, Bjork O, et al. Scandinavian Sarcoma Group Osteosarcoma Study SSG VIII: prognostic factors for outcome and the role of replacement salvage chemotherapy for poor histological responders. Eur J Cancer 2003;39:488–94.
21. Ferrari S, Smeland S, Mercuri M, Bertoni F, Longhi A, Ruggieri P, et al. Neoadjuvant chemotherapy with high-dose ifosfamide, high-dose methotrexate, cisplatin, and doxorubicin for patients with localized osteosarcoma of the extremity: a joint study by the Italian and Scandinavian sarcoma groups. J Clin Oncol 2005;23:8845–52.
22. Ferrari S, Mercuri M, Picci P, Bertoni F, Brach del Prever A, Tienghi A, et al. Nonmetastatic osteosarcoma of the extremity: results of a neoadjuvant chemotherapy protocol (IOR/OS-3) with high-dose methotrexate, intraarterial or intravenous cisplatin, doxorubicin, and salvage chemotherapy based on histologic tumor response. Tumori 1999;85:458–64.

Nucleophosmin as a Candidate Prognostic Biomarker of Ewing's Sarcoma Revealed by Proteomics

Kazutaka Kikuta,[1,5] Naobumi Tochigi,[2] Tadakazu Shimoda,[2] Hiroki Yabe,[5] Hideo Morioka,[5] Yoshiaki Toyama,[5] Ako Hosono,[3] Yasuo Beppu,[4] Akira Kawai,[4] Setsuo Hirohashi,[1] and Tadashi Kondo[1]

Abstract

Purpose: We aimed to identify novel prognostic biomarkers for Ewing's sarcoma by investigating the global protein expression profile of Ewing's sarcoma patients.

Experimental Design: We examined the proteomic profile of eight biopsy samples from Ewing's sarcoma patients using two-dimensional difference gel electrophoresis. Three patients were alive and continuously disease-free over 3 years after the initial diagnosis (good prognosis group) and five had died of the disease within 2 years of the initial diagnosis (poor prognosis group).

Results: The protein expression profiles produced using two-dimensional difference gel electrophoresis consisted of 2,364 protein spots, among which we identified 66 protein spots whose intensity showed >2-fold difference between the two patient groups. Mass spectrometric protein identification showed that the 66 spots corresponded to 53 distinct gene products. Pathway analysis revealed that 31 of 53 proteins, including nucleophosmin, were significantly related to bone tissue neoplasms ($P < 0.000001$). The prognostic performance of nucleophosmin was evaluated immunohistochemically on an additional 34 Ewing's sarcoma cases. Univariate and multivariate analyses revealed that nucleophosmin expression significantly correlated with overall survival ($P < 0.01$).

Conclusions: These results establish nucleophosmin as a candidate of independent prognostic marker for Ewing's sarcoma patients. Measuring nucleophosmin in biopsy samples before treatment may contribute to the effective management of Ewing's sarcoma.

Ewing's sarcoma is the second most common primary malignant bone tumor in children and adolescents. Despite significant progress regarding intensive chemotherapy protocols and local control measures, 30% to 40% of patients with localized Ewing's sarcoma and 80% of patients with metastatic Ewing's sarcoma at diagnosis die due to disease progression within 5 years (1). More intensified first-line chemotherapy regimens or combinations of chemotherapeutic agents improve clinical outcome compared with conventional chemotherapy (2, 3). However, such therapies may result in serious toxicity, including fatal gastrointestinal toxicity, grade 3 or 4 infections, and severe myelosuppression (4–6). The patients could thus benefit from less aggressive regimens by avoiding the higher risk of toxicity associated with overtreatment. Indeed, approximately two-thirds of patients with localized Ewing's sarcoma are cured with conventional therapy alone (7, 8). Therefore, the identification of prognostic factors may lead to the development of risk-adapted treatment strategies for Ewing's sarcoma.

Clinical factors currently evaluated have limited prognostic value; the presence of metastases at diagnosis, which is the most unfavorable prognostic factor for Ewing's sarcoma, concerns only ~25% of Ewing's sarcoma patients (9). The prognostic value of other clinical and pathologic features that correlated with prognosis of Ewing's sarcoma, including the site and size of the lesion and the age of the patient (1, 10), has decreased following recent advances in treatment (11). For instance, in earlier studies, tumors >8 cm were associated with a worse prognosis (12), whereas tumor size is not assumed as definitive prognostic factor in studies using the more intensive EW92 protocol (13).

In recent years, high-throughput screening technologies such as array-based comparative genomic hybridization analysis and cDNA microarray technology have been used to identify up-regulated or down-regulated genes with prognostic value for Ewing's sarcoma (14–19). These comprehensive studies suggested the presence of a poor prognosis signature at diagnosis and identified several genes that may be involved in the process of invasion and metastasis in Ewing's sarcoma.

Emerging technologies that examine the overall features of the expressed proteins, that is, proteomics, have identified many candidate proteins associated with early diagnosis (20),

Authors' Affiliations: [1]Proteome Bioinformatics Project, National Cancer Center Research Institute; [2]Diagnosis Pathology Division, [3]Pediatric Oncology Division, and [4]Orthopedic Surgery Division, National Cancer Center Hospital; [5]Department of Orthopedic Surgery, Keio University School of Medicine, Tokyo, Japan

Received 7/24/08; revised 12/17/08; accepted 1/10/09; published OnlineFirst 4/7/09.

Grant support: Ministry of Health, Labor and Welfare and Program for Promotion of Fundamental Studies in Health Sciences of the National Institute of Biomedical Innovation of Japan.

The costs of publication of this article were defrayed in part by the payment of page charges. This article must therefore be hereby marked *advertisement* in accordance with 18 U.S.C. Section 1734 solely to indicate this fact.

Note: Supplementary data for this article are available at Clinical Cancer Research Online (http://clincancerres.aacrjournals.org/).

Requests for reprints: Tadashi Kondo, Proteome Bioinformatics Project, National Cancer Center Research Institute, 5-1-1 Tsukiji, Chuo-ku, Tokyo 104-0045, Japan. Phone: 81-3-3542-2511, ext. 3004; Fax: 81-3-357-5298; E-mail: takondo@ncc.go.jp.

©2009 American Association for Cancer Research.

doi:10.1158/1078-0432.CCR-08-1913

Translational Relevance

In Ewing's sarcoma, a novel prognostic modality has long been desired to select the patients that would benefit from intensified treatment. We performed a proteomic study using incisionally biopsied samples before treatment. A comparative protein expression study in 8 patients identified nucleophosmin as a novel prognostic biomarker. A subsequent immunohistochemical study on a further 34 cases established the correlation between higher nucleophosmin expression and poor prognosis. In our study, nucleophosmin was identified as a novel candidate prognostic biomarker through the use of modern global protein expression modalities. Our study suggests the possible use of nucleophosmin expression for personalized medicine for Ewing's sarcoma patients.

differential diagnosis (21), prognosis (22, 23), and response to chemotherapy (24) in various diseases but have not been vigorously employed in the study of Ewing's sarcoma.

In this study, we performed a proteomic study using biopsy samples from Ewing's sarcoma patients. We found that nucleophosmin expression significantly correlated with progression of Ewing's sarcoma. Although aberrant expression of nucleophosmin has been implicated in various other malignancies (25–29), this proteomic study shows its aberrant expression and prognostic utility in Ewing's sarcoma.

Materials and Methods

Patients and clinical information. This study included a total of eight frozen incisional biopsy samples taken before treatment at the time of diagnosis from 8 Ewing's sarcoma patients treated between June 1996 and December 2006. These samples were snap-frozen in liquid nitrogen and stored at -80°C until use. The clinical information of the patients is summarized in Table 1. This project was approved by the ethical review board of the National Cancer Center after signed informed consent was obtained from all patients. All cases were reviewed and histopathologically diagnosed by a certified pathologist (N.T. and T.S.). Clinical staging was determined based on diagnostic imaging criteria according to the Musculoskeletal Tumor Society Surgical staging system (30). Primary tumor size was measured at the greatest tumor dimension on radiographic images, including computed tomography scans and magnetic resonance imaging.

From the 8 cases included in the study, 3 patients were alive and continuously disease-free (CDF) in the follow-up period of at least 3 years from diagnosis and 5 patients were dead of disease (DOD) within 2 years from initial diagnosis. All 5 patients in the latter group developed distant metastases within 7 months from initial diagnosis.

A previous report indicated that Ewing's sarcoma patients with early relapse, defined as relapse within 2 years after initial diagnosis, had shorter survival (31). We grouped the Ewing's sarcoma samples into two groups: the samples from patients that were alive and CDF over 3 years post-diagnosis were defined as the good prognosis group (Table 1, samples 1-3). The samples from patients that were DOD within 2 years were defined as the poor prognosis group (Table 1, samples 4-8).

For the nucleophosmin immunohistochemical expression study, we examined 34 tissues paraffin-embedded before treatment from 34 independent cases (Table 2, samples 9-42). These patients were treated between June 1981 and December 2005 at the National Cancer Center and Keio University Hospital. This project was approved by the ethical review boards of the National Cancer Center and Keio University Hospital after signed informed consent was obtained from all patients in this study. The clinical information concerning the cases used in the immunohistochemical study is summarized in Table 2.

Rearrangement analysis. Total RNA from tumors was extracted by the guanidinium thiocyanate method (ISOGEN, Nippon Gene). Samples were ground in a microcentrifuge tube. cDNA was generated using a first-strand cDNA synthesis kit (Pharmacia Biotech). Total RNA (1-5 μg) was transcribed. PCR was carried out in a 100 mL reaction mixture containing 1 to 7 μL cDNA template, 200 mmol/L deoxynucleotide triphosphates, 0.5 mmol/L of each oligonucleotide primer, and 2.5 units Taq polymerase in a 10 mmol/L Tris-HCl (pH 8.8) containing 50 mmol/L KCl and 1.5 mmol/L $MgCl_2$. The oligonucleotide primers used for the PCR were ESBP-1 (EWS specific), ESBP-2 (FLI-1 specific), and primers specific for ERG, E1AF, and ETV1 (32). PCR was done in 35 cycles under the following protocol: denaturation at 94°C for 1 min, annealing at 65°C for 1 min, and elongation at 72°C for 1 min. The amplified products were visualized on 1% agarose gels.

Protein expression profiling. Frozen samples were crushed to powder with a Multi-beads shocker (Yasui Kikai) with liquid nitrogen. The frozen powder was then treated with urea lysis buffer (6 mol/L urea, 2 mol/L thiourea, 3% CHAPS, 1% Triton X-100). After centrifugation at 15,000 rpm for 30 min, the supernatant was recovered and used in the subsequent protein expression studies.

Two-dimensional difference gel electrophoresis was done as described previously (33). In brief, the internal control sample was prepared by mixing a portion of all individual samples. Five micrograms of the internal control sample and of each individual sample were labeled with Cy3 and Cy5, respectively (CyDye DIGE Fluor saturation dye; GE Healthcare Biosciences) according to the manufacturer's instructions. The differently labeled protein samples were mixed and separated by two-dimensional difference gel electrophoresis. The first dimension separation was achieved using IPG DryStrip gels (24 cm

Table 1. Clinicopathologic features of the cases, the frozen samples of which were examined by proteomics

Case no.	Age/sex (y)	Primary site	Size (cm)	Sample source	Stage*	Metastatic site (first development)	Metastasis time after diagnosis (mo)	Follow-up period after diagnosis (mo)	Follow-up status
1	M/19	Thigh	8	Biopsy	L	None	None	88	CDF
2	F/18	Chest wall	4	Biopsy	L	None	None	70	CDF
3	F/9	Parietal Bone	4	Biopsy	L	None	None	46	CDF
4	M/62	Thigh	8	Biopsy	M	Lymph node, Brain	At diagnosis	12	DOD
5	F/28	Humerus	6	Biopsy	L	Lung	7	6	DOD
6	M/32	Thigh	15	Biopsy	M	Lung	At diagnosis	10	DOD
7	M/12	Ilium	11	Biopsy	L	Bone	7	7	DOD

*Stages I and II defined as localized disease (L) and stage III defined as metastatic disease (M).

length, pI range between 4 and 7; GE Healthcare Biosciences). The second dimension separation was achieved by SDS-PAGE on large-format gels (38 cm length, Bio-craft, Itabashi; ref. 33). The gels were scanned using laser scanners (Typhoon Trio; GE Healthcare Biosciences) at appropriate wavelengths (Fig. 1A). For all spots, the intensity of the Cy5 image was normalized by that of the Cy3 image in the identical gel so that gel-to-gel differences were compensated using the Progenesis PG240 software (Nonlinear Dynamics). System reproducibility was verified by comparing the protein profiles obtained from three independent separations of the same sample (Table 1, case 1). Scatter plot analysis revealed that the standardized intensity of >96.6% of the spots ranged within a 2-fold difference (R = 0.9103; Fig. 1B).

Protein identification by mass spectrometry. The proteins corresponding to the spots detected were identified using mass spectrometry according to our previous report (33). In brief, 100 μg Cy5- or Cy3-labeled proteins were separated by two-dimensional PAGE, recovered as gel plugs, and digested with modified trypsin (Promega). The trypsin digests were subjected to liquid chromatography (Paradigm MS4 dual solvent delivery system; Michrom BioResources) and mass spectrometry using a Finnigan LTQ linear ion trap mass spectrometer (Thermo Electron) equipped with a nano-electrospray ion source (AMR, Megro). The Mascot software (version 2.1; Matrix Science) was used to search for the mass of the peptide ion peaks against the SWISS-PROT database (*Homo sapiens*, 12867 sequence in Sprot_47.8 fasta file).

Functional classification of the identified proteins. Functional classification of the identified proteins was carried out according to their classification in Gene Ontology.[6]

Pathway analysis. Pathway analysis of the identified proteins was done using the MetaCore software analysis tool (GeneGo). MetaCore identifies networks based on a manually curated database containing known molecular interactions, functions, and disease interrelationships using proteome data. The pathways were identified by the probability that a random set of proteins with the same size as the input list would give rise to a particular mapping by chance. The identified networks were traced using the Metacore pre-filter tool. The Disease tab tool was used to automatically trace key proteins associated with disease networks stored in Metacore and to list the P value for each disease listed.

Immunohistochemical study. Nucleophosmin expression was examined immunohistochemically on paraffin-embedded tissues. In brief, 4-μm-thick tissue sections were autoclaved in 10 mmol/L citrate buffer (pH 6.0) at 121°C for 30 min and incubated with an antibody against nucleophosmin (sc-53175; Santa Cruz Biotechnology; 1:500 dilution) at room temperature. Immunostaining was done using the Envision Plus detection system (DAKO). Two observers (N.T. and K.K.) evaluated the staining in a blinded fashion for clinical data.

Statistical analysis. Hierarchical clustering was done using the Expressionist software (Genedata).

Statistical computations were done using the StatView version 5.0 statistical package (SAS Institute). Survival time was defined as the period from diagnosis to last follow-up (or death). Survival rate was estimated by the Kaplan-Meier method (34). The relationship between survival and other variables was investigated using the log-rank test for categorical variables and a score test based on the Cox proportional hazards model for continuous variables. A multivariate model was fitted using Cox regression with significant variables at the univariate level ($P < 0.01$; ref. 35). Following a large-scale cooperative study by the Japanese Musculoskeletal Oncology Group (36), in which age <16 years and tumor size <10 cm were shown to have a significantly worse clinical outcome by univariate survival analysis, we selected these cutoff values for this analysis.

[6] http://www.geneontology.org

Results

We generated and compared the protein expression profiles between three good prognosis and five poor prognosis Ewing's sarcoma cases using two-dimensional difference gel electrophoresis. We detected 2,364 protein spots that appeared in all the images of the Cy3-labeled internal control sample. Among these 2,364 spots, 66 showed significantly (>2-fold ratio of means) different intensity between the two groups. The localization of the 66 spots on the two-dimensional image is shown in Fig. 1C. Using hierarchical clustering, the 66 spots were classified into two major groups, cluster A (7 spots) and cluster B (59 spots; Fig. 2). The intensity of the 7 spots belonging to cluster A was decreased, whereas that of the 59 spots of cluster B was increased in the poor prognosis group.

Mass spectrometric analysis resulted in the identification of 53 distinct gene products (6 proteins in cluster A and 47 proteins in cluster B) corresponding to the 66 protein spots (Fig. 2; Supplementary Table S1).

Although all six proteins in cluster A belonged to different functional categories as classified in Gene Ontology, most of the proteins in cluster B were divided into eight main categories: cytoskeletal/structural protein, transcription/translation, signal transduction, transport, antiapoptosis, response oxidative stress, acute-phase response, and cell proliferation (Fig. 2).

We further explored the biological significance of the altered protein expression pattern in cluster B based on a manually curated database containing known molecular interactions, functions, and disease interrelationships using MetaCore. We found that 31 (65.9%) of 47 proteins were functionally linked with each other and that the identified network of the 31 proteins was significantly related to bone tissue neoplasms ($P < 0.000001$; Fig. 2).

In the 31 proteins of cluster B, nucleophosmin was included. Although aberrant expression of nucleophosmin has been implicated in various other malignancies (25–29), its association with Ewing's sarcoma has not been reported previously. Therefore, we validated the correlation of nucleophosmin with prognosis using immunohistochemistry in an additional 34 Ewing's sarcoma cases. Two patterns of nucleophosmin-positive staining were observed, both nuclear: a dot-like pattern and a diffuse-like pattern (Fig. 3). Similar to previous reports (25, 37), cases with nuclear staining for nucleophosmin were considered as nucleophosmin positive (23 of 34 cases; Table 2), whereas cases without staining for nucleophosmin were considered as nucleophosmin negative.

In the follow-up period (median, 57.5 months; range, 8-179 months), 13 of 34 patients were alive and CDF and 21 patients were DOD (Fig. 4A).

The group of nucleophosmin-positive cases included a significantly higher number of DOD patients compared with the nucleophosmin-negative group ($P < 0.01$, log-rank test; Fig. 4B), showing that nucleophosmin expression correlates with prognosis.

Following univariate analysis, nucleophosmin positivity ($P < 0.01$) and clinical stage (presence of metastatic disease at diagnosis; $P < 0.01$) significantly correlated with shorter overall survival. No other factors examined, including the tumor size, age at diagnosis, sex, chemotherapy regimens, tumor resectibility, and primary site, were associated with overall survival (Table 3).

Table 2. Clinicopathologic features of the 34 Ewing's sarcoma cases examined immunohistochemically

Case no.	Sex/age (y)	Primary site	Size (cm)	Sample source	Stage*	Metastatic site (first development)	Metastasis time after diagnosis (mo)	Follow-up period after diagnosis (mo)
9	M/9	Fibula	9	Biopsy	L	None	None	93
10	M/14	Clavicle	15	Biopsy	L	None	None	177
11	M/49	Femur	11	Biopsy	L	None	None	141
12	M/16	Arm	3	Biopsy	L	None	None	93
13	M/25	Rib	5.5	Biopsy	L	None	None	75
14	M/9	Talus	2	Biopsy	L	None	None	70
15	M/1	Tibia	—†	Biopsy	L	None	None	179
16	F/36	Femur	—†	Biopsy	L	None	None	174
17	M/13	Tibia	—†	Biopsy	L	None	None	166
18	F/22	Fibula	6	Biopsy	L	None	None	108
19	M/18	Rib	6.5	Biopsy	L	None	None	105
20	M/35	Thigh	8	Biopsy	L	None	None	126
21	F/36	Arm	4	Biopsy	L	None	None	101
22	M/15	Thigh	16	Biopsy	L	Lung	8	11
23	M/17	Rib	10	Biopsy	L	Multiple bone	7	8
24	M/18	Back	25	Biopsy	L	Lung	6	8
25	M/22	Femur	10	Biopsy	L	Bone	2	14
26	M/37	Ilium	25	Biopsy	M	Lung	At diagnosis	22
27	F/24	Sacrum	10	Biopsy	L	Bone	3	22
28	M/11	Femur	10	Biopsy	L	Bone, brain, lung	1	32
29	F/22	Humerus	18	Biopsy	L	Bone	19	32
30	F/20	Femur	5	Biopsy	L	Lung	41	75
31	M/21	Parietal bone	5	Biopsy	L	Lung	69	94
32	F/19	Humerus	7	Biopsy	L	Lung, bone	43	121
33	M/17	Vertebra	10	Biopsy	L	Lung	12	45
34	F/16	Tibia	20	Biopsy	M	Lung	At diagnosis	16
35	M/18	Fibula	7	Biopsy	L	Bone, lung	9	21
36	M/23	Pelvis	13	Biopsy	M	Lung	At diagnosis	17
37	M/29	Thigh	16	Biopsy	M	Chest	At diagnosis	12
38	F/63	Paravertebra	17	Biopsy	L	None	None	71
39	F/20	Lower leg	10	Biopsy	L	Lung, lymph node	9	14
40	F/56	Forearm	5	Biopsy	M	Lung	At diagnosis	11
41	M/7	Paravertebra	4	Biopsy	L	Brain	15	16
42	F/11	Paravertebra	6	Biopsy	L	Lung	17	22

NOTE: Chemotherapy agents: VACD, vincristine (VCR), actinomycin D (ACT), cyclophosphamide (CYC), and doxorubicin (DOX); IE, ifosfamide (IFO) and etoposide (ETO); THP, therarubicin; CDDP, cisplatin; BLM, bleomycin; MTX, methotrexate; DTIC, dacarbazine. NT, not tested.
*Stages I and II defined as localized disease (L) and stage III defined as metastatic disease (M).
†Tumor size cannot be evaluated.

We investigated whether nucleophosmin expression significantly correlated with the original tumor site and the tumor respectability status. Of the 34 cases in this study, 21 originated at an extra-axial and 13 at an axial site. Nucleophosmin expression did not correlate with the original tumor site (P = 0.87, Fisher's test). Of the 21 extra-axial tumors, 14 were nucleophosmin positive, and nucleophosmin expression correlated with poor prognosis ($P < 0.05$, log-rank test). Of the 13 axial tumors, 9 were nucleophosmin negative; again, nucleophosmin expression significantly correlated with poor prognosis ($P < 0.01$, log-rank test). Therefore, nucleophosmin expression correlated with poor prognosis independent of the original tumor site.

There was no significant difference regarding the prognosis between the resectable (26 of 34) and nonresectable cases (P = 0.1219, log-rank test). Among the resectable tumors, 16 were nucleophosmin positive and had worse prognosis than the remaining 10 nucleophosmin-negative tumors ($P < 0.01$, log-rank test).

Multivariate analysis done on nucleophosmin staining and clinical stage, identified as significant prognostic factors by univariate analysis, revealed that both significantly correlated, as separate variables, with overall survival (P = 0.0063; relative risk, 7.768; 95% confidence interval, 1.783-33.841 and P = 0.0039; relative risk, 5.964; 95% confidence interval, 1.773-20.060, respectively; Table 3).

On a second univariate analysis, we found that nucleophosmin positivity was also a strong negative predictor of overall survival in the 29 of 34 patients that had localized disease at diagnosis ($P < 0.01$; log-rank test; Fig. 4C).

Table 2. Clinicopathologic features of the 34 Ewing's sarcoma cases examined immunohistochemically (Cont'd)

Follow-up status	Nucleophosmin positivity	Fusion gene	Chemotherapy	Chemotherapy agents	Operation	Radiation
CDF	-	NT	VCD + I-based regimens	VCR, CYC, DOX, IFO, etc	Amputation	-
CDF	-	NT	VAIA	VCR, ACT, IFO, DOX	Wide resection	+
CDF	-	NT	VAIA	VCR, ACT, IFO, DOX	Wide resection	-
CDF	-	NT	VCD + I-based regimens	VCR, CYC, DOX, IFO, etc	Wide resection	-
CDF	-	NT	VCD + I-based regimens	VCR, CYC, DOX, IFO, etc	Wide resection	-
CDF	+	NT	VCD + I-based regimens	VCR, CYC, DOX, IFO, etc	-	+
CDF	+	NT	VAC	VCR, ACT, CYC	Amputation	+
CDF	-	NT	VACA	VCR, ACT, CYC, DOX	Amputation	+
CDF	-	EWS/ERG	CYVADIC	CYC, VCR, DOX, DTIC	Wide resection	+
CDF	-	EWS/FLI1 type 2	KS-1	ETO, CDDP, THP, IFO	Wide resection	-
CDF	-	EWS/FLI1 EWSex10/FLI-1ex6	KS-1	ETO, CDDP, THP, IFO	Wide resection	+
CDF	+	NT	KS-1	ETO, CDDP, THP, IFO	Wide resection	-
CDF	+	Not detected	KS-1	ETO, CDDP, THP, IFO	Wide resection	-
DOD	+	NT	National Cancer Institute protocol (VAC + IE)	VCR, DOX,CYC + IFO, ETO	Wide resection	+
DOD	+	EWS R1 rearrangement	ACT + CDDP	ACT, CDDP	-	+
DOD	+	NT	VACA	VCR, ACT, CYC, DOX	Intralesional resection	+
DOD	+	NT	VAIA	VCR, ACT, IFO, DOX	-	-
DOD	-	NT	National Cancer Institute protocol (VAC + IE)	VCR, DOX,CYC + IFO, ETO	-	+
DOD	+	NT	National Cancer Institute protocol (VAC + IE)	VCR, DOX,CYC + IFO, ETO	-	+
DOD	+	NT	VAC	VCR, ACT, CYC	Amputation	+
DOD	+	NT	VAIA	VCR, ACT, IFO, DOX	Wide resection	+
DOD	+	NT	T11	CYC, DOX,MTX, VCR + BLM, CYC, ACT + CYC, DOX, MTX	Wide resection	-
DOD	+	NT	National Cancer Institute protocol (VAC + IE)	VCR, DOX,CYC + IFO, ETO	-	+
DOD	+	NT	T11	CYC, DOX,MTX, VCR + BLM, CYC, ACT + CYC, DOX, MTX	-	+
DOD	+	NT	T11	CYC, DOX,MTX, VCR + BLM, CYC, ACT + CYC, DOX, MTX	Marginal resection	+
DOD	+	EWS/FLI1 type 2	KS-1	ETO, CDDP, THP, IFO	Wide resection	-
DOD	+	EWS/FLI1 type 1	KS-1	ETO, CDDP, THP, IFO	Wide resection	+
DOD	+	NT	KS-1	ETO, CDDP, THP, IFO	-	+
DOD	+	EWS/FLI1 type 2	KS-1	ETO, CDDP, THP, IFO	Intralesional resection	+
DOD	+	NT	KS-1	ETO, CDDP, THP, IFO	Intralesional resection	+
DOD	-	EWS/FLI1 type 1	KS-1	ETO, CDDP, THP, IFO	Marginal resection	+
DOD	+	NT	KS-1	ETO, CDDP, THP, IFO	Wide resection	-
DOD	+	Not detected	KS-1	ETO, CDDP, THP, IFO	Marginal resection	-
DOD	+	EWS/FLI1 type 1	KS-1	ETO, CDDP, THP, IFO	Intralesional resection	+

Discussion

The identification of novel prognostic biomarkers for Ewing's sarcoma is required to improve the management of Ewing's sarcoma. Global genomic and transcriptomic expression studies conducted to identify prognostic biomarkers for Ewing's sarcoma resulted in the identification of *MTA1*, *CDH11* (14), *STEAP1*, *NKX2-2*, and *CCND1* (15), gains in chromosomes 1q, 8, and 12 and deletions of 1p as genetic lesions implicated in the progression of Ewing's sarcoma (16–18). Although these comprehensive studies may have the potential to further increase our understanding of the biology of Ewing's sarcoma and to lead to the development of practical tumor markers to support individualized therapy, practical prognostic biomarkers of Ewing's sarcoma are presently not used in a clinical setting.

Proteomic studies have unique advantages on other omics studies. The proteome is a functional translation of the genome, directly regulating cell phenotypes, and is thus a rich source of biomarkers. With this notion, we have established the gel-based proteomics system for cancer research and applied it to the Ewing's sarcoma proteomic study presented here. This is the first report using a proteomic approach to develop prognostic biomarkers for Ewing's sarcoma.

We identified 6 down-regulated and 47 up-regulated proteins in Ewing's sarcoma cases with poor prognosis. Functional classification revealed that these identified proteins belonged to a variety of functional pathways, including cytoskeletal/structural organization, transcription/translation, signal transduction, transport, antiapoptosis, response-oxidative stress, acute-phase response, and cell proliferation. The results of functional classification may suggest that the proteomic alterations observed may be a part of global series of functionally interconnected molecular lesions that include transcriptional and translational aberrations, which, taken together, include both the causes and the results of carcinogenesis and cancer progression.

This proteome study identified or confirmed the presence of several molecular aberrations concerning Ewing's sarcoma. The

47 proteins found to be up-regulated included neuron-specific enolase, which has been found to be associated with poor prognosis in Ewing's sarcoma (38, 39).

Nucleophosmin was included in the 47 proteins found to be up-regulated. Nucleophosmin overexpression has been related to carcinogenesis and tumor progression in prostate (25), gastric (26), colon (27), ovarian (28), and urinary bladder carcinomas (29). However, the association of nucleophosmin with Ewing's sarcoma has not been reported previously, including, importantly, in previous genomic and transcriptomic studies of Ewing's sarcoma (14–19). This may be due to discordance between mRNA and protein expression, the fact

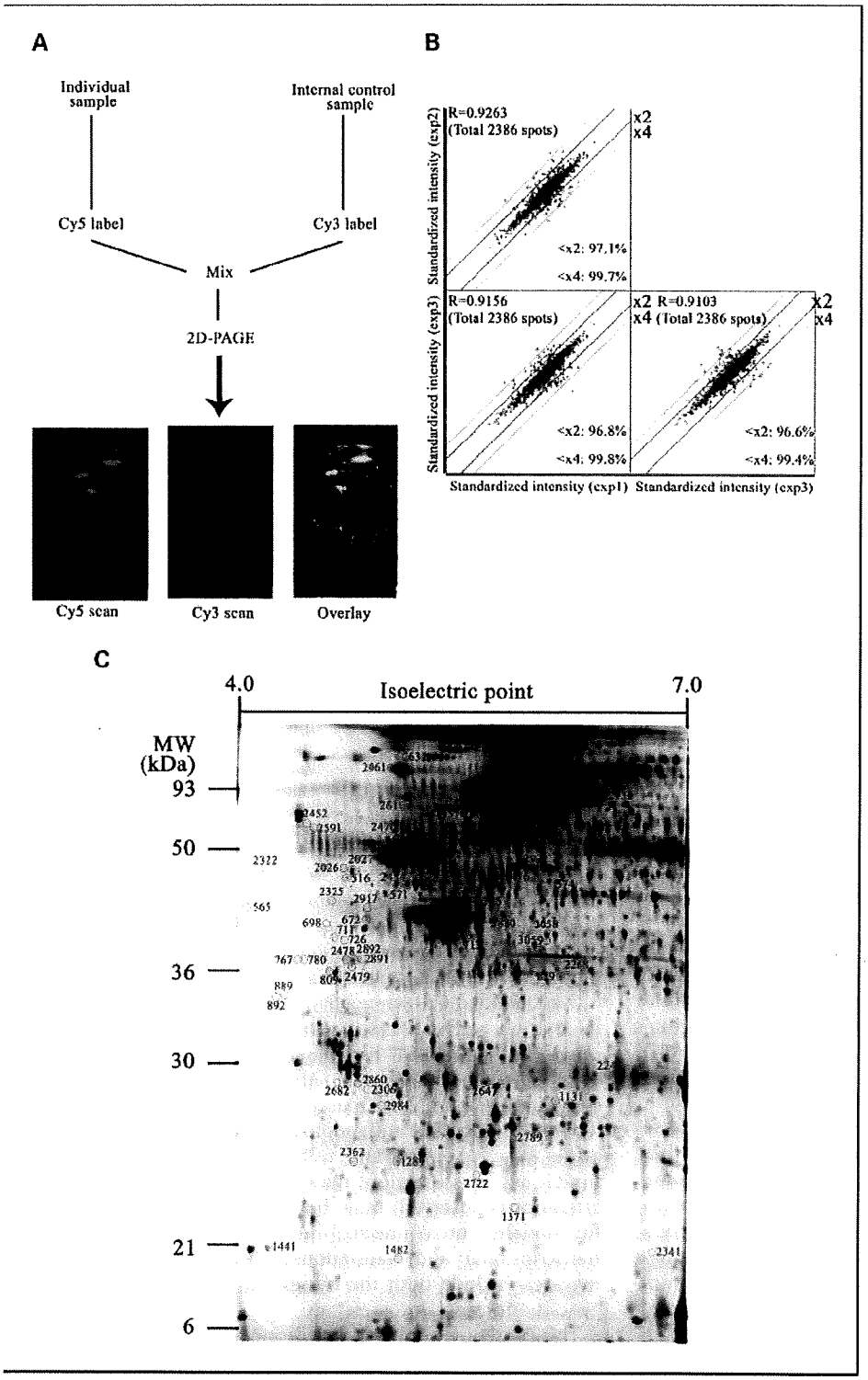

Fig. 1. Identification of proteins differentially expressed in Ewing's sarcoma. *A*, schematic workflow of sample preparation for quantitative analysis. Protein lysates are labeled with fluorescent dyes of different wavelengths of excitation and emission. Cy3-labeled samples are simultaneously mixed and divided into Cy5-labeled samples. Then, mixture of Cy3- and Cy5-labeled lysates are coseparated by two-dimensional difference gel electrophoresis. The gel is scanned with two wavelengths, each specific either for Cy3 or Cy5 dye. *B*, scattergram of expression profile of Ewing's sarcoma tissues. Comparison of data from three independent experiments revealed the high reproducibility of protein expression profiling. *C*, representative two-dimensional image of proteins detected in Ewing's sarcoma tissues. The 66 spots identified in this study are circled and numbered. The spot numbers correspond to those in Fig. 2 and Supplementary Table S1.

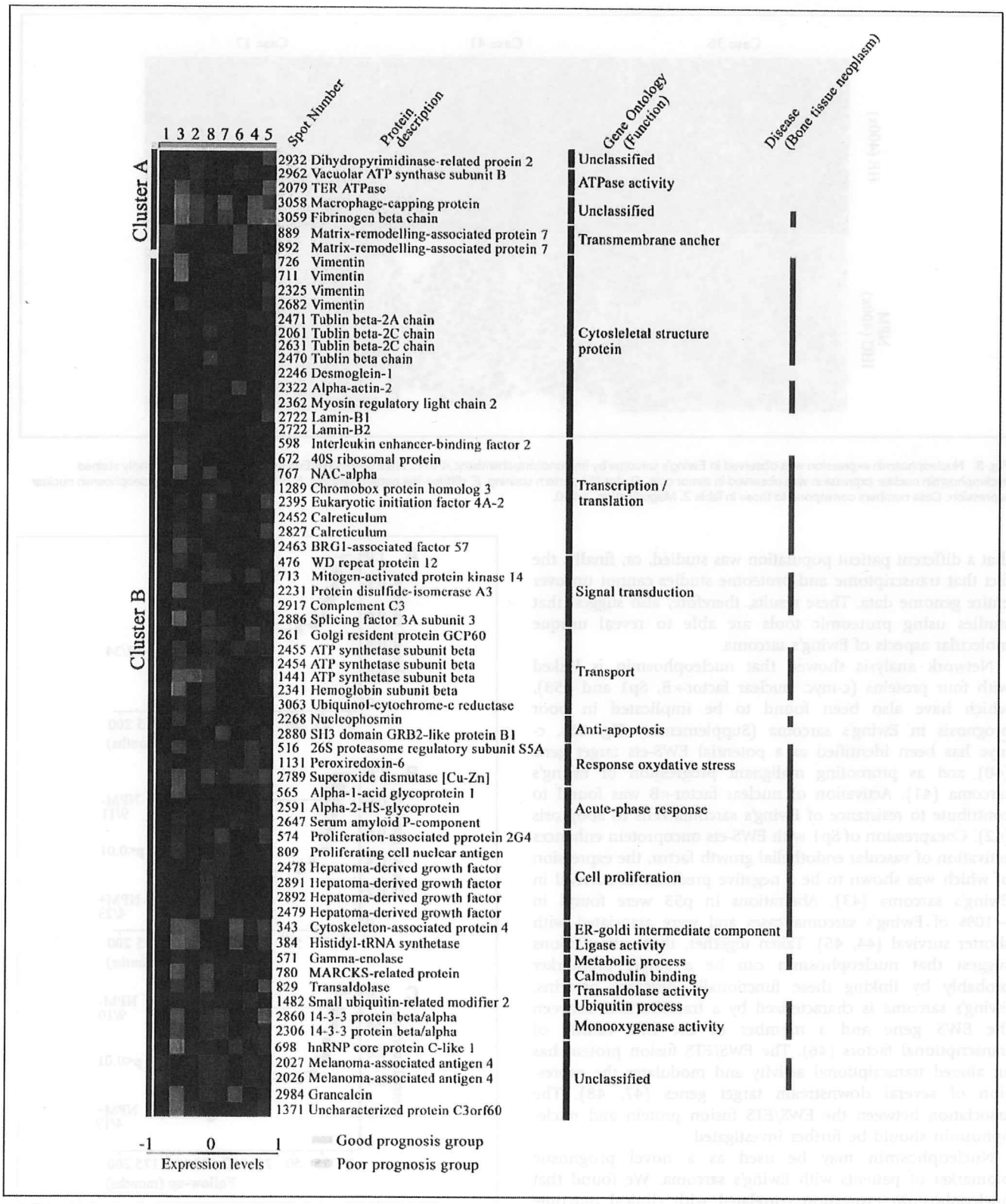

Fig. 2. Hierarchical clustering of the 8 Ewing's sarcoma cases based on the intensity of the 66 protein spots detected. The cases are color-coded as yellow (good prognosis group) or light blue (poor prognosis group). The spot numbers, protein names, Gene Ontology (functional classification), and disease (bone tissue neoplasms; color-coded as red) related proteins are shown (*right*).

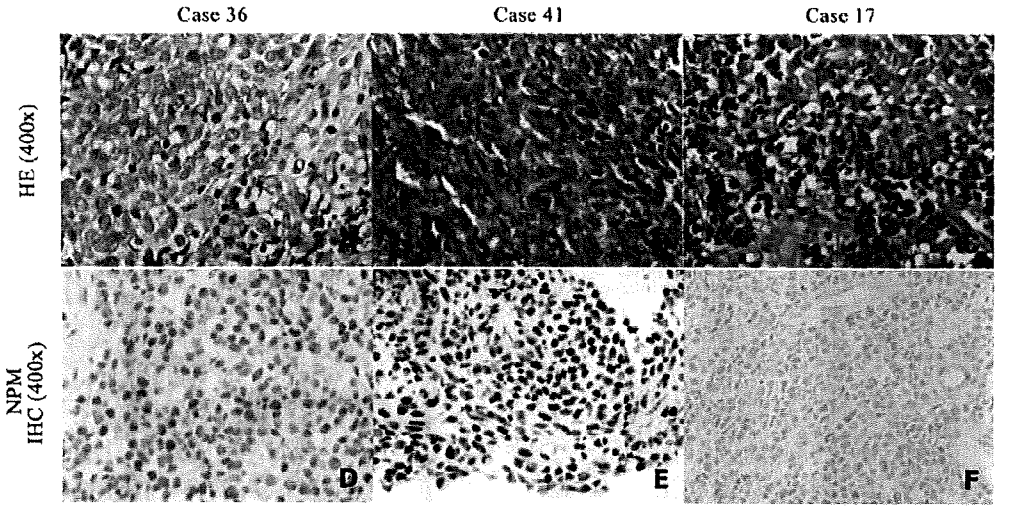

Fig. 3. Nucleophosmin expression was observed in Ewing's sarcoma by immunohistochemistry. *A* to *C*, H&E staining of Ewing's sarcoma cases. Strongly stained nucleophosmin nuclear expression was observed in tumor cells. *D*, dot-like pattern staining. *E*, diffuse-like pattern staining. *F*, not observed stained nucleophosmin nuclear expression. Case numbers correspond to those in Table 2. Magnification, ×400.

that a different patient population was studied, or, finally, the fact that transcriptome and proteome studies cannot uncover entire genome data. These results, therefore, also suggest that studies using proteomic tools are able to reveal unique molecular aspects of Ewing's sarcoma.

Network analysis showed that nucleophosmin is linked with four proteins (c-myc, nuclear factor-κB, Sp1 and p53), which have also been found to be implicated in poor prognosis in Ewing's sarcoma (Supplementary Fig. S1). c-myc has been identified as a potential EWS-ets target gene (40) and as promoting malignant progression of Ewing's sarcoma (41). Activation of nuclear factor-κB was found to contribute to resistance of Ewing's sarcoma cells to apoptosis (42). Coexpression of Sp1 with EWS-ets oncoprotein enhances activation of vascular endothelial growth factor, the expression of which was shown to be a negative predictor of survival in Ewing's sarcoma (43). Aberrations in p53 were found in ~10% of Ewing's sarcoma cases and were associated with shorter survival (44, 45). Taken together, these observations suggest that nucleophosmin can be a single biomarker probably by linking these functionally different proteins. Ewing's sarcoma is characterized by a translocation between the *EWS* gene and a member of the *ETS* family of transcriptional factors (46). The EWS/ETS fusion protein has an altered transcriptional activity and modulates the expression of several downstream target genes (47, 48). The association between the EWS/ETS fusion protein and nucleophosmin should be further investigated.

Nucleophosmin may be used as a novel prognostic biomarker of patients with Ewing's sarcoma. We found that nucleophosmin expression correlated with clinical outcome in 34 Ewing's sarcoma patients. Univariate and multivariate analyses revealed that nucleophosmin expression along with clinical stage (presence of metastases at diagnosis) was an independent prognostic factor in Ewing's sarcoma patients. Furthermore, nucleophosmin expression was also a significant

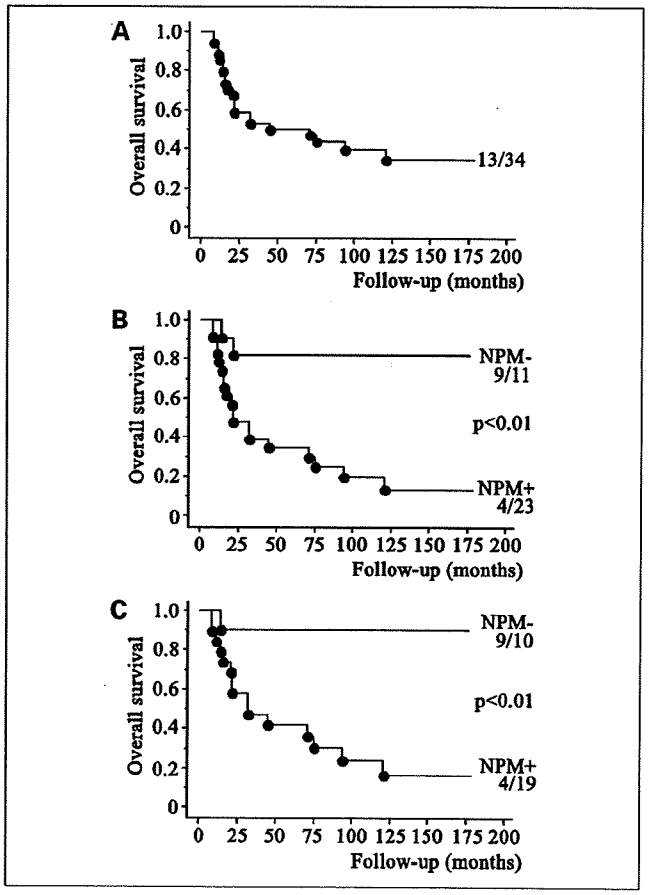

Fig. 4. Kaplan-Meier estimated overall survival curves are illustrated for all patients ($n = 34$; *A*), for all patients based on nucleophosmin positivity (*B*), and for patients with localized disease ($n = 29$) by nucleophosmin positivity (*C*). Statistically significant differences in overall survival periods were observed between the nucleophosmin-positive and nucleophosmin-negative cases both for all cases ($P < 0.01$, log-rank test) and the cases with localized disease ($P < 0.01$, log-rank test).

Table 3. Univariate and multivariate analyses of prognostic factors

Variable	Univariate survival analysis				Multivariate survival analysis	
	No. cases	No. alive	Univariate *P*	Risk ratio (95% confidence interval)	*P*	Relative risk (95% confidence interval)
Age at diagnosis (y)						
<16	9	5	0.3209	1		
≥16	25	8		1.738 (0.583-5.180)		
Sex						
M	22	10	0.5325	1		
F	12	3		0.517 (0.207-1.288)		
Primary site						
Extremity	21	10	0.212	1		
Axial	13	3		1.736 (0.730-4.126)		
Tumor size (cm)*						
<10	16	7	0.0182	1		
≥10	15	2		2.952 (1.202-7.251)		
Clinical stage						
Localized	29	13	<0.01	1	0.0039	1
Metastatic	5	0		5.238 (1.697-16.164)		5.964 (1.773-20.060)
Chemotherapy regimens						
Including IE	17	4	0.0629	1		
Not including IE	17	9		0.425 (0.955-5.791)		
Tumor resectibility						
Resectable	26	12	0.1219	1		
Nonresectable	8	1		2.004 (0.200-1.244)		
Nucleophosmin immunohistochemistry						
Negative	11	9	<0.01	1	0.0063	1
Positive	23	4		7.425 (1.715-32.147)		7.768 (1.783-33.841)

*Tumor size could not be evaluated in 3 Ewing's sarcoma cases.

prognostic factor in patients with localized disease. Applying these findings in a clinical setting poses the next challenge. As the incisional biopsy is a procedure done routinely in establishing the diagnosis in Ewing's sarcoma, the immunohistochemical examination of nucleophosmin expression can be done without any additional invasive examinations.

Although previous reports have suggested a possible association between nucleophosmin and malignancies, the functional role of nucleophosmin in Ewing's sarcoma is still unclear. Nucleophosmin overexpression has been reported to be involved in human tumorigenesis (49, 50). In one study, it led to increased proliferation and inhibition of apoptosis in tumor cells; overexpression of nucleophosmin reduced the percentage of cells in the G_1 phase and increased the S-phase population in the p53-negative cells but induced cell cycle arrest in normal cells. Conducting further basic research on the function of nucleophosmin will pave the way for further understanding of the molecular background of Ewing's sarcoma and, hopefully, for novel diagnostic and therapeutic applications.

In conclusion, global protein expression profiling revealed the proteomic background of Ewing's sarcoma and identified novel associations of several proteins with progression of Ewing's sarcoma. Of the proteins with expression that may have prognostic value, we successfully validated the association of nucleophosmin expression with poor prognosis. The expression of the other proteins may still have prognostic value and further validation studies may prove it. Evaluation of nucleophosmin expression may allow the identification of poor prognosis Ewing's sarcoma patients who may benefit from highly effective treatment in the future.

Disclosure of Potential Conflicts of Interest

No potential conflicts of interest were disclosed.

Acknowledgments

We thank Chizu Kina and Sachiko Miura for excellent technical support in the immunohistochemical study and Yukiko Fujie for excellent technical support in electrophoresis.

References

1. Cotterill SJ, Ahrens S, Paulussen M, et al. Prognostic factors in Ewing's tumor of bone: analysis of 975 patients from the European Intergroup Cooperative Ewing's Sarcoma Study Group. J Clin Oncol 2000; 18:3108–14.
2. Atra A, Whelan JS, Calvagna V, et al. High-dose busulphan/melphalan with autologous stem cell rescue in Ewing's sarcoma. Bone Marrow Transplant 1997;20:843–6.
3. Diaz MA, Vicent MG, Madero L. High-dose busulfan/melphalan as conditioning for autologous PBPC transplantation in pediatric patients with solid tumors. Bone Marrow Transplant 1999;24:1157–9.
4. Bernstein ML, Devidas M, Lafreniere D, et al. Intensive therapy with growth factor support for patients with Ewing tumor metastatic at diagnosis: Pediatric Oncology Group/Children's Cancer Group Phase II Study 9457—a report from the Children's Oncology Group. J Clin Oncol 2006;24:152–9.
5. Engelhardt M, Zeiser R, Ihorst G, Finke J, Muller CI. High-dose chemotherapy and autologous peripheral

blood stem cell transplantation in adult patients with high-risk or advanced Ewing and soft tissue sarcoma. J Cancer Res Clin Oncol 2007;133:1–11.
6. McTiernan A, Driver D, Michelagnoli MP, Kilby AM, Whelan JS. High dose chemotherapy with bone marrow or peripheral stem cell rescue is an effective treatment option for patients with relapsed or progressive Ewing's sarcoma family of tumours. Ann Oncol 2006; 17:1301–5.
7. Grier HE, Krailo MD, Tarbell NJ, et al. Addition of ifosfamide and etoposide to standard chemotherapy for Ewing's sarcoma and primitive neuroectodermal tumor of bone. N Engl J Med 2003;348:694–701.
8. Kolb EA, Kushner BH, Gorlick R, et al. Long-term event-free survival after intensive chemotherapy for Ewing's family of tumors in children and young adults. J Clin Oncol 2003;21:3423–30.
9. Paulussen M, Ahrens S, Burdach S, et al. Primary metastatic (stage IV) Ewing tumor: survival analysis of 171 patients from the EICESS studies. European Intergroup Cooperative Ewing Sarcoma Studies. Ann Oncol 1998;9:275–81.
10. Bacci G, Ferrari S, Bertoni F, et al. Prognostic factors in nonmetastatic Ewing's sarcoma of bone treated with adjuvant chemotherapy: analysis of 359 patients at the Istituto Ortopedico Rizzoli. J Clin Oncol 2000; 18:4–11.
11. Rodriguez-Galindo C, Spunt SL, Pappo AS. Treatment of Ewing sarcoma family of tumors: current status and outlook for the future. Med Pediatr Oncol 2003;40:276–87.
12. Hayes FA, Thompson EI, Meyer WH, et al. Therapy for localized Ewing's sarcoma of bone. J Clin Oncol 1989;7:208–13.
13. Marina NM, Pappo AS, Parham DM, et al. Chemotherapy dose-intensification for pediatric patients with Ewing's family of tumors and desmoplastic small round-cell tumors: a feasibility study at St. Jude Children's Research Hospital. J Clin Oncol 1999;17:180–90.
14. Ohali A, Avigad S, Zaizov R, et al. Prediction of high risk Ewing's sarcoma by gene expression profiling. Oncogene 2004;23:8997–9006.
15. Cheung IY, Feng Y, Danis K, et al. Novel markers of subclinical disease for Ewing family tumors from gene expression profiling. Clin Cancer Res 2007;13: 6978–83.
16. Armengol G, Tarkkanen M, Virolainen M, et al. Recurrent gains of 1q, 8 and 12 in the Ewing family of tumours by comparative genomic hybridization. Br J Cancer 1997;75:1403–9.
17. Maurici D, Perez-Atayde A, Grier HE, Baldini N, Serra M, Fletcher JA. Frequency and implications of chromosome 8 and 12 gains in Ewing sarcoma. Cancer Genet Cytogenet 1998;100:106–10.
18. Hattinger CM, Potschger U, Tarkkanen M, et al. Prognostic impact of chromosomal aberrations in Ewing tumours. Br J Cancer 2002;86:1763–9.
19. Schaefer KL, Eisenacher M, Braun Y, et al. Microarray analysis of Ewing's sarcoma family of tumours reveals characteristic gene expression signatures associated with metastasis and resistance to chemotherapy. Eur J Cancer 2008;44:699–709.
20. Petricoin EF, Ardekani AM, Hitt BA, et al. Use of proteomic patterns in serum to identify ovarian cancer. Lancet 2002;359:572–7.
21. Suehara Y, Kondo T, Fujii K, et al. Proteomic signatures corresponding to histological classification and grading of soft-tissue sarcomas. Proteomics 2006;6: 4402–9.
22. Chen G, Gharib TG, Wang H, et al. Protein profiles associated with survival in lung adenocarcinoma. Proc Natl Acad Sci U S A 2003;100:13537–42.
23. Suehara Y, Kondo T, Seki K, et al. Pfetin as a prognostic biomarker of gastrointestinal stromal tumors revealed by proteomics. Clin Cancer Res 2008;14: 1707–17.
24. Okano T, Kondo T, Fujii K, et al. Proteomic signature corresponding to the response to gefitinib (Iressa, ZD1839), an epidermal growth factor receptor tyrosine kinase inhibitor in lung adenocarcinoma. Clin Cancer Res 2007;13:799–805.
25. Subong EN, Shue MJ, Epstein JI, Briggman JV, Chan PK, Partin AW. Monoclonal antibody to prostate cancer nuclear matrix protein (PRO:4-216) recognizes nucleophosmin/B23. Prostate 1999;39: 298–304.
26. Tanaka M, Sasaki H, Kino I, Sugimura T, Terada M. Genes preferentially expressed in embryo stomach are predominantly expressed in gastric cancer. Cancer Res 1992;52:3372–7.
27. Nozawa Y, Van Belzen N, Van der Made AC, Dinjens WN, Bosman FT. Expression of nucleophosmin/B23 in normal and neoplastic colorectal mucosa. J Pathol 1996;178:48–52.
28. Zhang Y. The ARF-B23 connection: implications for growth control and cancer treatment. Cell Cycle 2004;3:259–62.
29. Tsui KH, Cheng AJ, Chang PL, Pan TL, Yung BY. Association of nucleophosmin/B23 mRNA expression with clinical outcome in patients with bladder carcinoma. Urology 2004;64:839–44.
30. Wolf RE, Enneking WF. The staging and surgery of musculoskeletal neoplasms. Orthop Clin North Am 1996;27:473–81.
31. Shankar AG, Ashley S, Craft AW, Pinkerton CR. Outcome after relapse in an unselected cohort of children and adolescents with Ewing sarcoma. Med Pediatr Oncol 2003;40:141–7.
32. Urano F, Umezawa A, Yabe H, et al. Molecular analysis of Ewing's sarcoma: another fusion gene, EWS-E1AF, available for diagnosis. Cancer Sci 1998;89: 703–11.
33. Kondo T, Hirohashi S. Application of highly sensitive fluorescent dyes (CyDye DIGE Fluor saturation dyes) to laser microdissection and two-dimensional difference gel electrophoresis (2D-DIGE) for cancer proteomics. Nat Protoc 2006;1:2940–56.
34. Kaplan EL, Meier P. Nonparametric estimation from incomplete observations. J Am Stat Assoc 1958;53:1.
35. Cox DR. Regression models and life tables. J R Stat Soc 1972;34:187–220.
36. Obata H, Ueda T, Kawai A, et al. Clinical outcome of patients with Ewing sarcoma family of tumors of bone in Japan: the Japanese Musculoskeletal Oncology Group cooperative study. Cancer 2007;109: 767–75.
37. Yun JP, Miao J, Chen GG, et al. Increased expression of nucleophosmin/B23 in hepatocellular carcinoma and correlation with clinicopathological parameters. Br J Cancer 2007;96:477–84.
38. Bacci G, Ferrari S, Bertoni F, et al. Neoadjuvant chemotherapy for peripheral malignant neuroectodermal tumor of bone: recent experience at the Istituto Rizzoli. J Clin Oncol 2000;18:885–92.
39. Oberlin O, Deley MC, Bui BN, et al. Prognostic factors in localized Ewing's tumours and peripheral neuroectodermal tumours: the third study of the French Society of Paediatric Oncology (EW88 study). Br J Cancer 2001;85:1646–54.
40. Bailly RA, Bosselut R, Zucman J, et al. DNA-binding and transcriptional activation properties of the EWS-FLI-1 fusion protein resulting from the t(11;22) translocation in Ewing sarcoma. Mol Cell Biol 1994;14: 3230–41.
41. Sollazzo MR, Benassi MS, Magagnoli G, et al. Increased c-myc oncogene expression in Ewing's sarcoma: correlation with Ki67 proliferation index. Tumori 1999;85:167–73.
42. Javelaud D, Poupon MF, Wietzerbin J, Besancon F. Inhibition of constitutive NF-κB activity suppresses tumorigenicity of Ewing sarcoma EW7 cells. Int J Cancer 2002;98:193–8.
43. Fuchs B, Inwards CY, Janknecht R. Vascular endothelial growth factor expression is up-regulated by EWS-ETS oncoproteins and Sp1 and may represent an independent predictor of survival in Ewing's sarcoma. Clin Cancer Res 2004;10:1344–53.
44. Abudu A, Mangham DC, Reynolds GM, et al. Overexpression of p53 protein in primary Ewing's sarcoma of bone: relationship to tumour stage, response and prognosis. Br J Cancer 1999;79: 1185–9.
45. de Alava E, Antonescu CR, Panizo A, et al. Prognostic impact of P53 status in Ewing sarcoma. Cancer 2000;89:783–92.
46. Delattre O, Zucman J, Plougastel B, et al. Gene fusion with an ETS DNA-binding domain caused by chromosome translocation in human tumours. Nature 1992;359:162–5.
47. Ladanyi M. EWS-FLI1 and Ewing's sarcoma: recent molecular data and new insights. Cancer Biol Ther 2002;1:330–6.
48. Siligan C, Ban J, Bachmaier R, et al. EWS-FLI1 target genes recovered from Ewing's sarcoma chromatin. Oncogene 2005;24:2512–24.
49. Itahana K, Bhat KP, Jin A, et al. Tumor suppressor ARF degrades B23, a nucleolar protein involved in ribosome biogenesis and cell proliferation. Mol Cell 2003;12:1151–64.
50. Grisendi S, Mecucci C, Falini B, Pandolfi PP. Nucleophosmin and cancer. Nat Rev Cancer 2006; 6:493–505.

 DOI 10.1002/prca.200800168 *Proteomics Clin. Appl.* 2009, *3*, 584–596

RESEARCH ARTICLE

Anatomic site-specific proteomic signatures of gastrointestinal stromal tumors

Yoshiyuki Suehara[1, 2, 3], Kazutaka Kikuta[1, 2, 4], Robert Nakayama[2, 4, 5], Kiyonaga Fujii[1], Hitoshi Ichikawa[5], Tatsuhiro Shibata[6], Kunihiko Seki[7]**, Tadashi Hasegawa[7]***, Masahiro Gotoh[8], Naobumi Tochigi[8], Tadakazu Shimoda[7], Yasuhiro Shimada[9], Takeshi Sano[10], Yasuo Beppu[2], Hisashi Kurosawa[3], Setsuo Hirohashi[1], Akira Kawai[2] and Tadashi Kondo[1]*

[1] Proteome Bioinformatics Project, National Cancer Center Research Institute, Tokyo, Japan
[2] Orthopedics Surgery Division, National Cancer Center Hospital, Tokyo, Japan
[3] Department of Orthopedic Surgery, Juntendo University, Tokyo, Japan
[4] Department of Orthopedic Surgery, Keio University, Tokyo, Japan
[5] Cancer Transcriptome Project, National Cancer Center Research Institute, Tokyo, Japan
[6] Cancer Genomics Project, National Cancer Center Research Institute, Tokyo, Japan
[7] Clinical Laboratory Division, National Cancer Center Hospital, Tokyo, Japan
[8] Pathology Division, National Cancer Center Research Institute, Tokyo, Japan
[9] Gastrointestinal Oncology Division, National Cancer Center Hospital, Tokyo, Japan
[10] Gastric Surgery Division, National Cancer Center Hospital, Tokyo, Japan

The gastrointestinal stromal tumor (GIST) is the most common mesenchymal malignancy of the gastrointestinal tract. Its clinical course ranges widely from a curable disorder to a highly malignant disease. Although its clinical and molecular characteristics depend on the anatomic site of origin, the molecular background of GIST arising in different anatomical site has not been studied yet. To investigate the proteomic background of GIST, we examined the proteomic features corresponding to the anatomic site of tumor origin. Comparison of the proteomic profile of gastric (23 cases) and small intestinal (9 cases) GIST by 2-DE revealed 105 protein spots with significantly different intensity ($p < 0.01$) between the two groups. Mass spectrometric study identified 68 distinct proteins for these 105 protein spots, including cancer-associated ones such as prohibitin, pigment epithelium-derived factor, and alpha-actinin 4. The intensity of 37/105 (35.2%) protein spots was significantly concordant with the corresponding mRNA levels ($p < 0.01$). Although both 2-D DIGE and microarray experiments showed significant up-regulation of vimentin expression in small intestinal GIST, Western blotting did not show a significant difference between the two groups. In conclusion, our study demonstrates the proteins specially expressed in GIST depending on their site of origin, as well as the unique advantage offered by use of proteomics to acquire such data. The identified proteins may provide clues to understanding the different characteristics of GIST depending on their site of origin.

Received: July 28, 2008
Revised: October 20, 2008
Accepted: November 3, 2008

Keywords:
2-D DIGE / Anatomic site / Gastrointestinal stromal tumor / Proteomics

Correspondence: Dr. Tadashi Kondo, Proteome Bioinformatics Project, National Cancer Center Research Institute, 5-1-1 Tsukiji, Chuo-ku, Tokyo 104-0045, Japan
E-mail: takondo@ncc.go.jp
Fax: +81-3-3547-5298

Abbreviation: GIST, gastrointestinal stromal tumor

* Present address: Department of Structural Biology, Graduate School of Pharmaceutical Sciences, Hokkaido University, Sapporo, Japan
** Present address: Department of Pathology, Japan Railway Tokyo General Hospital, Tokyo, Japan;
*** Present address: Department of Clinical Pathology, Sapporo Medical University School of Medicine, Sapporo, Japan

© 2009 WILEY-VCH Verlag GmbH & Co. KGaA, Weinheim

1 Introduction

The gastrointestinal stromal tumor (GIST) is the most common primary mesenchymal malignancy of the gastrointestinal tract [1, 2]. While the clinical course of GIST ranges widely from a curable disorder to a highly malignant disease, the molecular background of its malignant behavior is largely obscure.

GIST is characterized by the mutation of c-kit and PDGFR, and molecular targeting therapy using imatinib, a tyrosine kinase inhibitor originally developed for the treatment of chronic myeloblastic leukemia, has been proven effective in the treatment of GIST patients. Imatinib has also been shown to suppress the metastasis of GIST post surgery. However, as severe side effects of imatinib treatment have been reported, novel diagnostic modalities to select the patients with poor prognosis before treatment are needed in order to refine current therapeutic strategies. We recently identified pfetin as a novel prognostic biomarker for personalized medicine for GIST patients; by measuring pfetin expression in primary tumor tissues, we can predict the probability for metastasis post surgery [3]. Research avenues to translate these results to clinical application are currently under consideration in our laboratory.

The clinical and molecular characteristics of the GIST tumors depend on the anatomic site of origin. For example, the malignant behavior of GIST has been significantly correlated with the anatomical site of origin; the clinical course of small intestinal GIST is more aggressive than that of gastric ones [4, 5]. Investigation of the molecular background of tumors arising in different anatomical sites through "omics" studies may lead to the development of biomarkers to predict the prognostic biomarker for GIST patients and to novel therapeutic strategies. An array CGH study revealed the presence of site-dependent DNA copy number patterns, including the frequent loss of 1p and 15q in small intestinal and gastric GIST, respectively [6]. A global mRNA expression study resulted in the identification of anatomic site-specific genes, including those involved in muscle contraction and development, modulators for digestive enzymes, cell-cycle regulators, growth factor receptors and mediators of growth factor signaling [7]. Similarly, following mRNA expression studies, connexin 43, a gap junction protein, was extensively studied and was found to be uniquely expressed in small intestinal GIST [8]. Recent reports indicated the presence of mutations in the insulin-like growth factor receptor and BRAF genes [9, 10]. The investigation of genes specific to the anatomic site of origin may provide clues to understanding the molecular background of GIST.

In this report, we conducted a proteomic study to investigate the proteins the expression of which is associated with the site of origin of GIST. The 2-D DIGE detected 105 protein spots that had significantly different intensity between GIST tissues from different anatomic sites. MS identified the proteins corresponding to these 105 protein spots, and their expression levels were compared with their mRNA expression levels as detected by a DNA microarray. To further examine the potential clinical application of our findings, we examined the expression of certain identified proteins, such as vimentin using specific antibodies, and compared the results with those obtained by the proteomic and transcriptomic assays.

2 Materials and methods

2.1 Surgical specimens and clinical information

We examined the tumor tissues from 36 GIST patients who underwent surgery at the National Cancer Center Hospital consecutively from October 1977 to December 2005. All patients underwent resection with curative intent, and were not treated with adjuvant chemotherapy. Pathological diagnosis was based on the WHO classification system for soft-tissue tumors [11, 12], and included the examination of tumor size, presence of necrosis, degree of differentiation, mitotic rate, MIB-1 index, presence of epithelioid cells, and CD34 and CD117 expression. The clinical and pathological data concerning the patients are summarized in Table 1 and Supporting Information Table 1. Consistent with a previous report, c-kit mutations in exon 11 were more frequently observed in the gastric GIST [13-15]. Other factors did not show significant differences between the gastric and small intestinal GIST. This project was approved by the institutional review board of the National Cancer Center.

2.2 2-D DIGE and data analysis

The protein expression profiles were obtained by 2-D DIGE as previously described [3]. In brief, frozen tissues were crushed to powder by CryoPress (Microtech Nichion, Chiba, Japan) under cooling conditions. The frozen powder was then dissolved in a urea lysis buffer containing 6 M urea, 2 M thiourea, 3% CHAPS and 1% Triton X-100. Five micrograms of the protein samples was labeled with CyDye DIGE Fluor saturation dye (GE Healthcare, Uppsala, Sweden). The internal control sample, which was composed of a mixture of small portions of all samples examined in this experiment, was labeled with Cy3 fluorescence dye, while the individual samples were labeled with Cy5 fluorescence dye. These differently labeled protein samples were mixed and co-separated by 2-D PAGE. The first dimension separation was achieved on immobiline dry strip (IPG) gels (24-cm length, *pI* range between 4 and 7, GE Healthcare), and the second separation by SDS-PAGE on 9–16% gradient gels using EttanDalt II (GE Healthcare). Gel images were obtained by scanning the gels with a laser scanner (Typhoon Trio, GE Healthcare) (Supporting Information Fig. 1A). The Cy5 intensity was normalized by the Cy3 intensity in the identical gel for all protein spots using image analysis software (DeCyder version 4.0, GE Healthcare). The data were exported from DeCyder to the Expressionist data-mining package

© 2009 WILEY-VCH Verlag GmbH & Co. KGaA, Weinheim

Table 1. Clinicopathologic features of the training and validation set samples

	Learning set			Validation set
	Stomach	Small intestine		Stomach
	$n = 23$	$n = 9$	*P* value	$n = 4$
Age	59.9 ± 10.6	65.7 ± 13.5	0.207[a]	66.0 ± 6.0
Gender			0.761[b]	
Male	14	6		2
Female	9	3		2
Histology			0.454[b]	
Spindle	17	6		4
Mixed	4	3		0
Epithelioid	2	0		0
***c-Kit* Mutation**			0.003[b]	
Exon 9	0	4		0
Exon 11	16	3		3
Wild type	7	2		1
Risk classification			0.416[b]	
High	13	4		1
Intermediate	7	2		1
Low	3	3		2
Tumor size (cm)			0.374[b]	
<5cm	5	4		2
5-10cm	8	3		1
>10cm	10	2		1
MIB-1 grading			0.709[b]	
Grade 1	12	5		3
Grade 2	8	2		0
Grade 3	3	2		1

a) Student's *t*-test.
b) Chi-square test.

(GeneData, Basel, Switzerland), to identify the protein spots with statistically different intensity between the sample groups. System reproducibility was verified by running an identical sample three times. Scatter plot analysis revealed that the correlation coefficiency between the independent experiments was more than 0.92 and that the intensity of more than 97% of the protein spots was scattered within a twofold difference range (Supporting Information Fig. 1B). The significance of differences in spot intensity was evaluated using the Wilcoxon test. Hierarchical clustering, principal component analysis (PCA), correlation matrix analysis and spot ranking were performed using the Expressionist software.

2.3 MS protein identification

Protein identification was achieved by MS as previously described [3]. In brief, 100 μg of each protein sample was labeled with Cy5 fluorescence dye and separated by 2-D PAGE. The protein spots were recovered by an automated robot (SpotPiker, GE Healthcare Biosciences, UK). The proteins in the recovered spots were treated with modified trypsin (Promega, Madison, WI) and extracted as trypsin digests, which were then separated by micro-flow HPLC (Paradigm MS4 dual solvent delivery system, Michrom BioResources, Auburn, CA), and subjected to MS/MS (Finnigan LTQ linear IT mass spectrometer, Thermo Electron, San Jose, CA) equipped with a nano-electrospray ion source (AMR, Tokyo, Japan). The MASCOT software (version 2.1, Matrix science, London, UK) was used to search for the mass of the peptide ion peaks against the Swiss-Prot database (*Homo sapiens*, 12 867 sequences in Sprot_47.8 fasta file). Proteins with a MASCOT score of 35 or more were selected for identification. When multiple proteins were identified in a single spot, the proteins with the highest number of peptides were considered as those corresponding to the spot.

© 2009 WILEY-VCH Verlag GmbH & Co. KGaA, Weinheim

2.4 DNA microarray

DNA microarray data were obtained from the same samples and deposited in a public database (Gene Expression Omnibus, accession number GSM202197-202228). The procedures followed for the gene expression study are described in the Gene Expression Omnibus database (http://www.ncbi.nlm.nih.gov/geo/).

2.5 c-kit and PDGFRA mutation studies

The tumor tissues were examined for the mutation status of the c-kit and PDGFRA genes in our previous study [3].

2.6 Western blotting

The expression of vimentin was examined employing a specific antibody. Using 10 μg of each of the protein samples, the samples were separated by SDS-PAGE, transferred onto an NC membrane and incubated with a mouse mAb against vimentin (1:200 dilution, Sigma-Aldrich, Saint Louis, MO) and a HRP-conjugated secondary antibody (1:1000 dilution, GE Healthcare Biosciences). The immune complex was detected by enhanced chemiluminescence (ECL, GE Healthcare) and LAS-3000 (Fuji Film, Tokyo). The relative expression level of vimentin was normalized with that of actin in the same samples using ImageQuant TL software (GE Healthcare).

3 Results

3.1 Overall features of protein expression of GIST tissues

The protein expression profiles of 36 primary GIST were generated employing 2-D DIGE. Altogether, 1411 protein spots were observed in more than 75% of Cy3 images of the internal control sample, and these protein spots were selected to be further examined. Although potentially resulting in loss of information, this trimming process decreased the possibility of irrelevant expression data being studied. The overall features of the proteome were investigated by unsupervised classification methods such as hierarchical clustering analysis (Supporting Information Fig. 1C) and PCA (Supporting Information Fig. 1D). The GIST tissue samples were not clearly separated according to their site of origin based on the intensity of these 1411 protein spots.

3.2 Proteins differentially expressed in gastric and small intestinal GIST

We used 32 of the 36 samples to find the proteins that are differentially expressed in gastric and small intestinal GIST; mRNA expression data were also available for these 32 samples. We then used the remaining four samples to validate the results. We identified 105 protein spots the intensity of which was statistically different ($p < 0.01$) between the gastric (23 cases) and small intestinal (9 cases) GIST. The location of the 105 spots on the 2-D images is shown in Supporting Information Figs. 1A and 2. The GIST samples were separated according to their site of origin based on the intensity of these 105 protein spots using hierarchical clustering (Fig. 1A and Supporting Information Fig. 3) and PCA (Fig. 1B). Correlation matrix analysis revealed that the intensity pattern of the 105 protein spots was similar for GIST tumors of the same site of origin (Fig. 1C). We then examined the four remaining gastric GIST samples, and found that they were clustered with the other gastric GIST samples in hierarchical clustering (Fig. 1D and Supporting Information Fig. 4 for an enlarged image and its heat map) and PCA (Supporting Information Fig. 5).

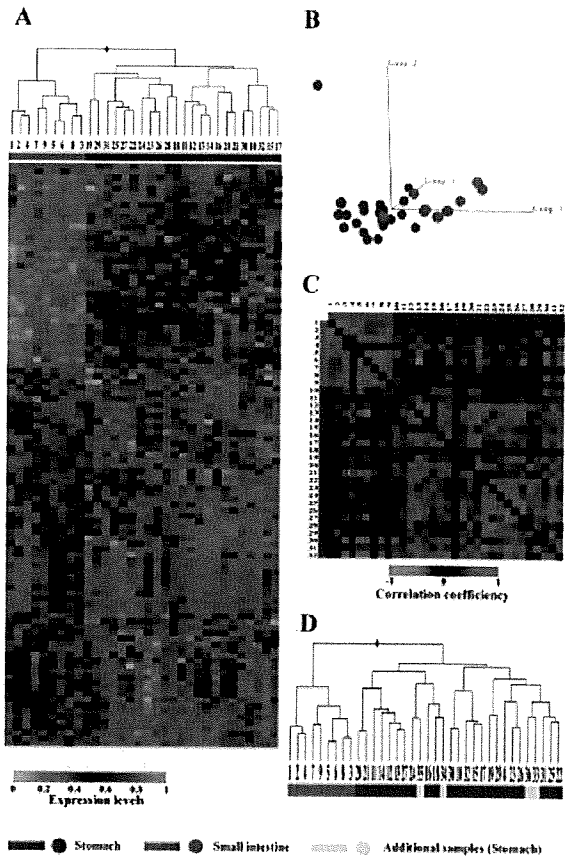

Figure 1. Protein spots with different intensity between the two groups of GIST arising in different anatomic sites. The GIST samples are were grouped based on the intensity of the 105 protein spots by (A) hierarchical clustering and (B) PCA, showing that the samples were grouped according to their anatomic site of origin based on the intensity of 105 protein spots. (C) Correlation matrix demonstrates the sample heterogeneity based on the intensity of the 105 protein spots. (D) An additional four GIST samples of stomach origin were examined by hierarchical clustering to confirm the results. All four samples were fairly classified.

© 2009 WILEY-VCH Verlag GmbH & Co. KGaA, Weinheim